

Supporting Information

Graphite/ amorphous diamond coupled frames with high ORR and OER performance apply to zinc-air batteries cathode catalyst

S1 Chemical reagent

Boracic acid ($\geq 95\%$)、Chitosan (deacetylation degree $\geq 95\%$), Glacial acetic acid from Aladdin (100%) and Pluronic F-127 ($\geq 99.5\%$) from Shanghai yuanye Bio-Technology Co, Ltd .

S2 Materials Characterizations

The crystal structure information of as-prepared catalysts was obtained from X-ray diffraction (XRD, DX-2700) using Cu K α radiation with a scan speed of 4° min^{-1} . The specific XRD parameters are as follows

target	= Cu (0.154056 nm)
voltage	= 40.0 (kV)
current	= 30.0 (mA)

Describe the morphology structure of catalysts by field emission scanning electron microscopy (SEM, SIGMA500) and transmission electron microscopy (TEM, JEOL JEM-2100). (SEM and TEM sample preparation: First, a sample of 1mg was taken, followed by adding 1 mL of anhydrous ethanol and ultrasonic oscillation for 30 min. Use a pipette gun to measure 20 μL of liquid, drip onto the cleaned silicon wafer, and then dry with an infrared lamp.)

The chemical state of the sample was determined by X-ray photoelectron spectroscopy (XPS, ESCALAB 250XI). (First of all, 15 mg samples were weighed and mixed into $3\times 3\text{mm}$ tablets by a tablet press. In the sample preparation process, we used double-sided tape to glue the samples to the aluminum foil to avoid signal interference

caused by the aluminum foil tape not being covered.)

The graphitization degree of the samples was measured by Raman spectroscopy (Thermo Scientific DXR 3Xi). Raman's test wavelength is 532 nm. Sample handling: The powder sample should be flattened with a glass slide before testing to obtain a flat surface.

S3 The potential of Hg/HgO is related to RHE

In this paper, all electrochemical tests have been normalized via conversion to a standard reversible hydrogen potential.

$$E (RHE) = E (Hg/HgO) + 0.0592pH + 0.098$$

S4 ORR Measurements

The number of electron transfers in ORR (oxygen reduction reaction) can be calculated using the K-L equation.

$$\frac{1}{J} = \frac{1}{J_L} + \frac{1}{J_K} = \frac{1}{B\omega^{0.5}} + \frac{1}{J_K}$$
$$B = 0.2nFC_o(D_0)^{2/3}\nu^{-1/6}$$

where J is the limit current density tested, J_k is the kinetic limiting current density, J_L is the diffusion-limited current density, n is the number of electron transfers, F is Faraday's constant (96485 C mol⁻¹), ω is the angular velocity of the rotating disk electrode in rpm, C_o is the volume concentration of O₂ (1.6×10⁻⁶ mol cm⁻³), D_0 is the diffusion coefficient of O₂ in 0.1 mol L⁻¹ KOH (1.9×10⁻⁵ cm² s⁻¹), and K is the electron transfer rate (when the ω unit is rpm, $K=0.2$), ν is the kinematic viscosity (0.01 cm² s⁻¹)

1).

The yield of H_2O_2 in the ORR reaction using the rotating disk electrode (RRDE) technique can be calculated as follows:

$$\%H_2O_2 = 200 \frac{I_R/N}{I_D + I_R/N}$$

The electron transfer number (n) is calculated as follows:

$$n = 4 \frac{I_D}{I_R/N + I_D}$$

Where I_R indicates the ring current and I_D indicates the disk current. N is 0.37.

S5 Calculation of Effective Active Surface Area (ECSA)

The electrochemically active surface area (ECSA) of the electrochemical double-layer capacitor (C_{DL}) can be evaluated using the cyclic voltammetry (CV) method. The double-layer capacitance can be obtained by scanning at 10, 20, 30, 30, 40, and 50 mV s^{-1} .

$$C_{DL} = \frac{i_m}{v} = (i_a - i_c)/2v$$

$$ECSA = C_{DL}/C_s$$

Where C_{DL} is the double layer capacitor (mF), the average current of the i_m working electrode, i_c , and i_a represents the cathode and anode current (mA) respectively, v represents the scanning rate ($V s^{-1}$) C_s is the specific capacitance of the catalyst ($mF cm^{-2}$). It is generally considered to be $0.035 mF cm^{-2}$ in 0.1 M KOH electrolyte.

S6 OER Measurements

The OER test is performed in a 0.1M KOH solution, and nitrogen is injected to remove oxygen from the solution.

The catalytic performance of the biofunctional catalyst ($\Delta E = E_{j=10} - E_{1/2}$) is determined by the difference between the potential corresponding to the oxygen evolution reaction with 10 mA cm^{-2} ($E_{j=10}$) for OER and the half-wave potential of the oxygen reduction reaction ($E_{1/2}$).

S7 Zn-air Batteries

The zinc-air batteries described in this paper were tested in a 6 M KOH solution. In these batteries, the polished zinc sheet acted as the negative electrode, while the carbon cloth coated with the catalyst acted as the positive electrode. The cycle test was performed at 5 mA cm^{-2} , with a charging time of 5 minutes and a discharging time of 5 minutes for each cycle.

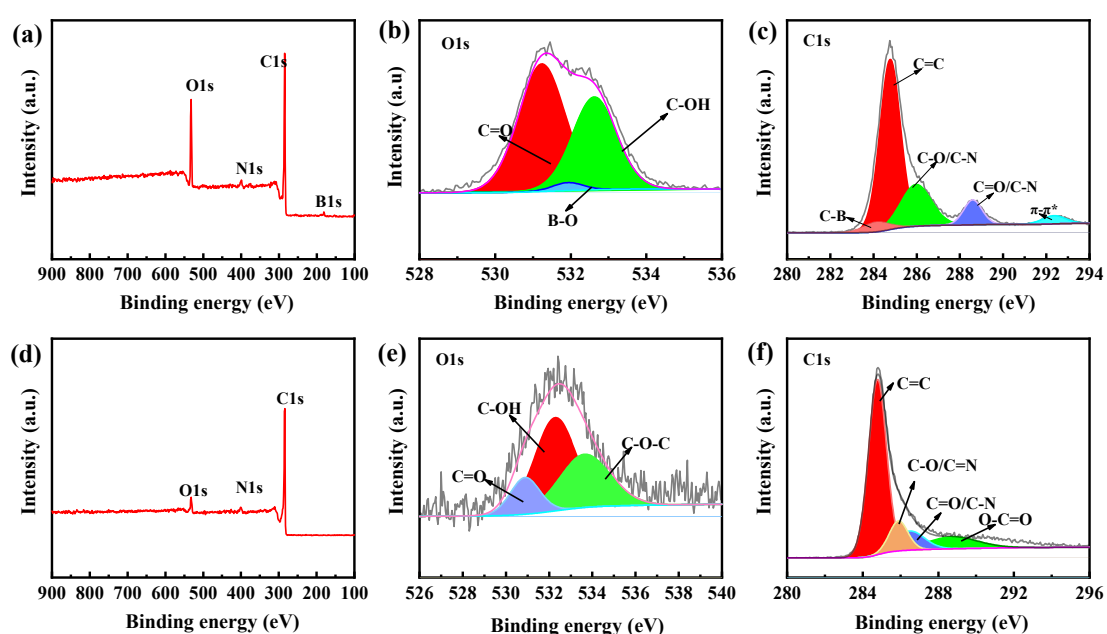


Figure S1 XPS of CSF127B₁.(a) Total spectrum. (b)O1s. (c) C1s.

XPS of CSF127. (d) Total spectrum. (e)O1s. (f) C1s.

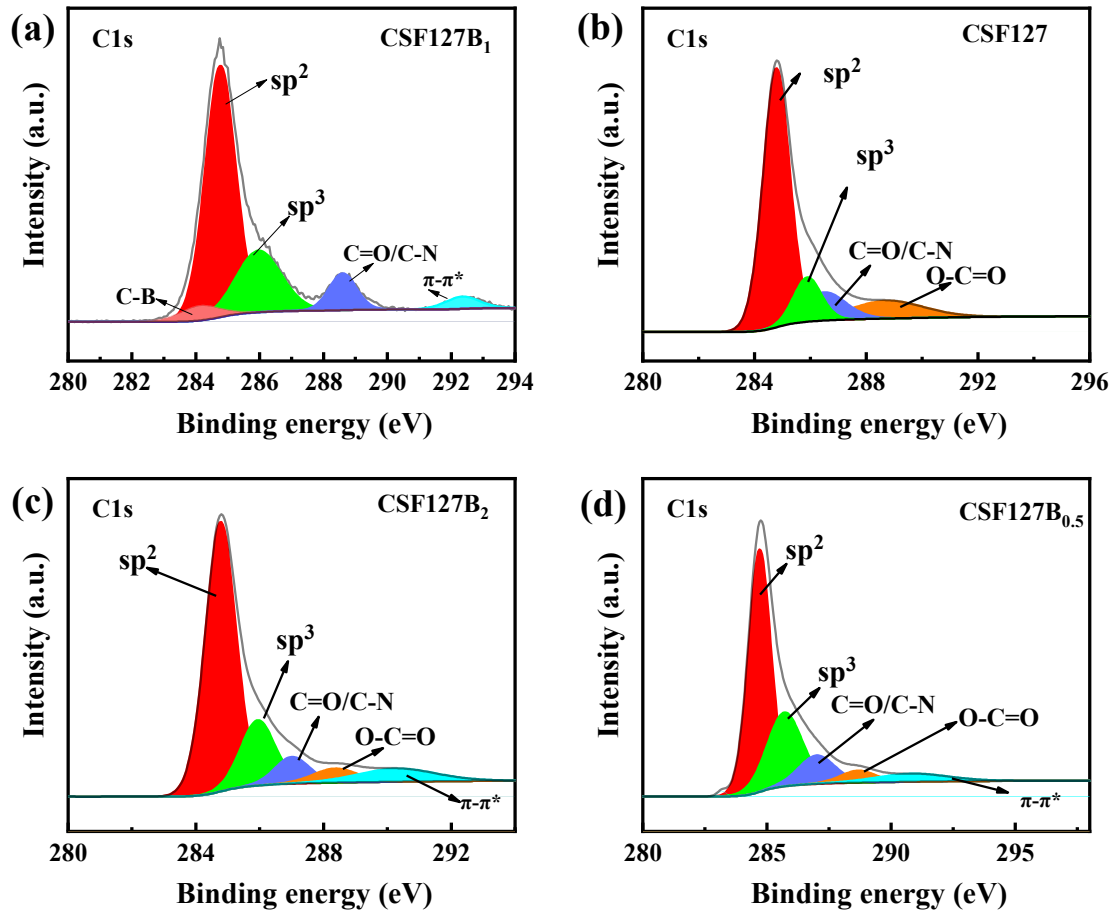


Figure S2 Deconvolution of the C 1s core level spectra for samples (a)CSF127B₁;(b)CSF127;(c)CSF127B₂;(d)CSF127B_{0.5}

Table S1 Different sample element content

	B (at%)	C(at%)	N(at%)	O(at%%)
CSF127B ₁	2.06	84.23	2.27	11.44
CSF127	0	90.21	4.02	5.77
CSF127B _{0.5}	1.32	87.76	4.51	6.41
CSF127B ₂	1.2	87.3	5.33	6.17

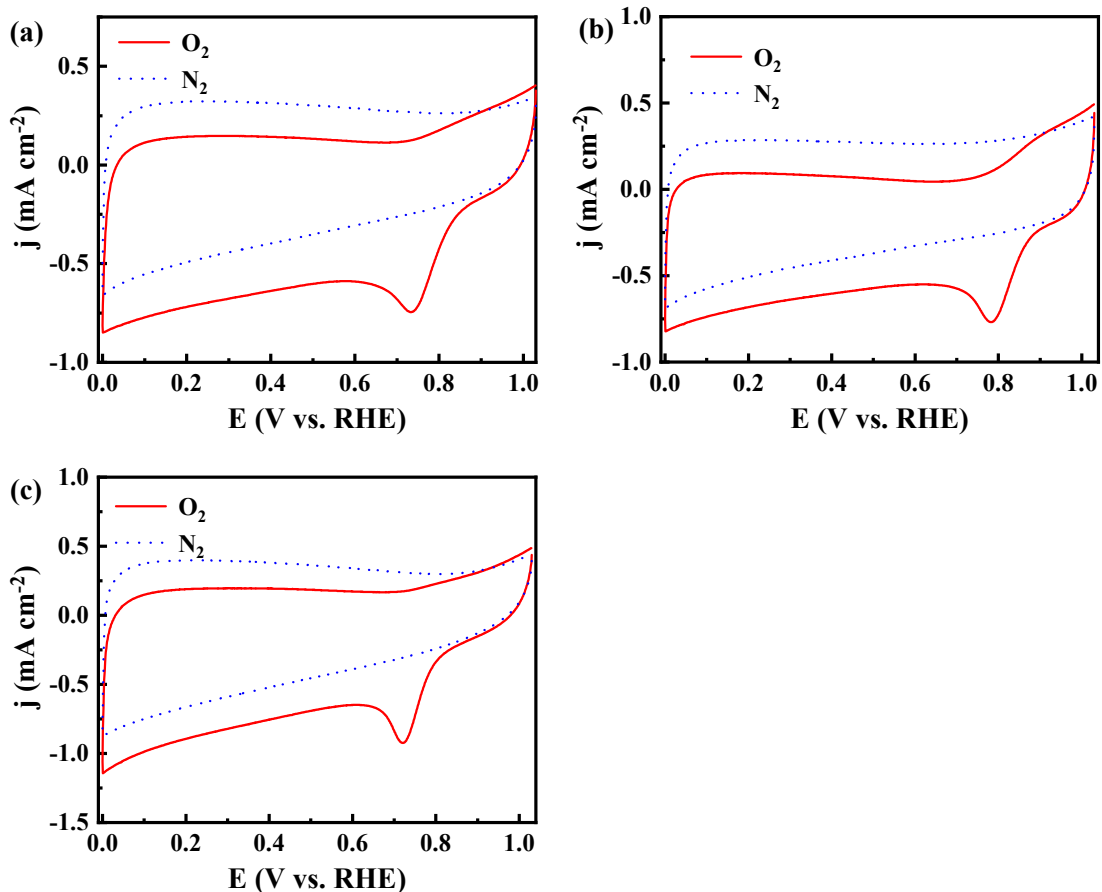


Figure S3 (a) CVs of CSF127B_{0.5}.(b) CVs of CSF127 .(c) CVs of CSF127B₂ in O₂ and N₂-saturated 0.1 M KOH solution.

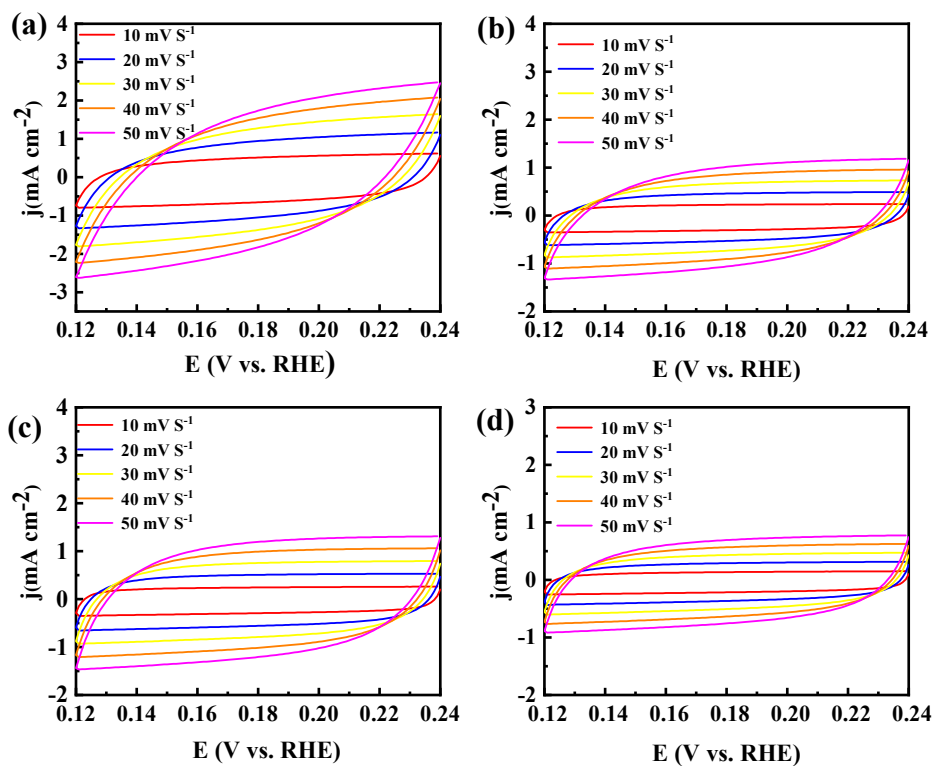


Figure S4 10-50 mV s⁻¹ CV curves at different sweep speeds (a) CSF127B₁.

(b)CSF127.(c)CSF127B₂.(d)CSF127B_{0.5}.

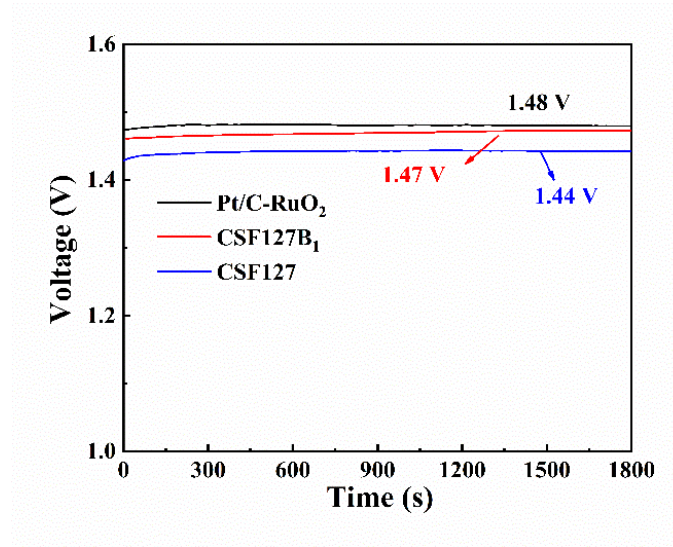


Figure S5 Open circuit voltage of CSF127B₁, CSF127 and Pt/C-RuO₂ in Zinc-air battery.

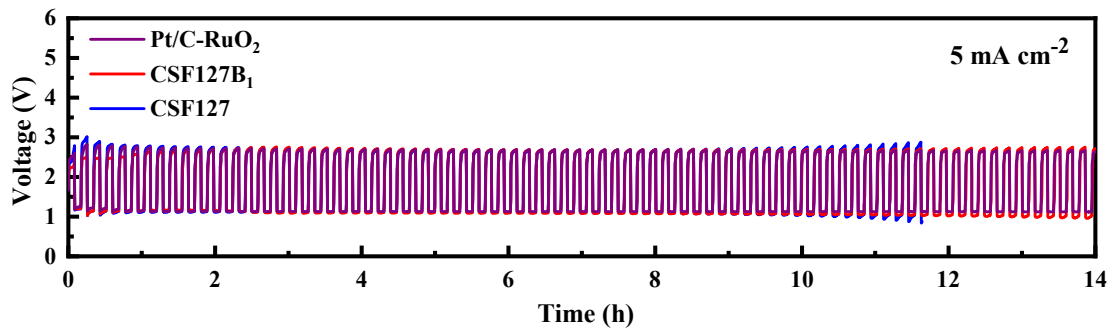


Figure S6 Zooming of zinc-air battery cycle

Table S2 Comparison of ORR and OER properties of different catalysts

Catalyst	onset potential (V)	ORR Performance $E_{1/2}$ (V)	Limiting current Density (mA cm ⁻²)	OER Performance $E_{j=10}$	ΔE ($E_{j=10}-E_{1/2}$) (V)	Ref
CSF127B ₁	0.924	0.821	5.26	1.515	0.694	This work
NBCNT-10	0.958	0.82	5.52	—	—	1
BN-C-1	0.876	0.812	5.88	—	—	2
BN/C	—	0.8	5	—	—	3
N _{0.54} -Z ₃ /M ₁ -900	0.94	0.824	—	—	—	4
NPSCS	0.965	0.834	6.04	1.662	0.828	5
CNT@NSCF	0.94	0.82	—	1.56	0.74	6
NBF-CNW	0.95	0.818	6	—	—	7
B,N-Carbon	0.98	0.84	6	1.57	0.73	8
NPBC	0.98	0.86	—	1.68	0.82	9
NB-CN	0.92	0.84	—	1.65	0.81	10
SHG	1.01	0.87	5.01	1.56	0.77	11

References

1. P. Wei, X. Li, Z. He, X. Sun, Q. Liang, Z. Wang, C. Fang, Q. Li, H. Yang, J. Han and Y. Huang, *Chemical Engineering Journal*, 2021, **422**.
2. M. Fan, Q. Yuan, Y. Zhao, Z. Wang, A. Wang, Y. Liu, K. Sun, J. Wu, L. Wang and J. Jiang, *Advanced Materials*, 2022, **34**.
3. R. Zhao, Q. Li, Z. Chen, V. Jose, X. Jiang, G. Fu, J.-M. Lee and S. Huang, *Carbon*, 2020, **164**, 398-406.
4. X. Li, B. Y. Guan, S. Gao and X. W. Lou, *Energy & Environmental Science*, 2019, **12**, 648-655.
5. X. Tao, Q. Zhang, Y. Li, X. Lv, D. Ma and H.-g. Wang, *Applied Surface Science*, 2019, **490**, 47-55.
6. X. Wang, G.-L. Li, Z.-F. Lu, S. Cao, C. Hao, S. Wang and G. Sun, *Catalysis Science & Technology*, 2022, **12**, 181-191.
7. Z. Lu, Z. Li, S. Huang, J. Wang, R. Qi, H. Zhao, Q. Wang and Y. Zhao, *Applied Surface Science*, 2020, **507**.
8. T. Sun, J. Wang, C. Qiu, X. Ling, B. Tian, W. Chen and C. Su, *Advanced Science*, 2018, **5**.
9. b. Qiaodi Wanga, Yiming Lic, Kai Wanga, Juntao Zhoua, Lianwen Zhuc, Li Gua, Jing Hub, Xuebo Cao, *Electrochimica Acta*, 2017, **257**, 250-258.
10. Z. Lu, J. Wang, S. Huang, Y. Hou, Y. Li, Y. Zhao, S. Mu, J. Zhang and Y. Zhao, *Nano Energy*, 2017, **42**, 334-340.
11. C. Hu and L. Dai, *Advanced Materials*, 2016, **29**.